Bending stresses in Facetted Glass Shells

Anne Bagger, Jeppe Jönsson, Henrik Almegaard
Technical University of Denmark, Institute of Civil Engineering, Denmark,
aeb@byg.dtu.dk, www.byg.dtu.dk

A shell structure of glass combines a highly effective structural principle with a material of optimal permeability to light. A facetted shell structure has a piecewise plane geometry, and together the facets form an approximation to a curved surface. A distributed load on a plane-based facetted structure will locally cause bending moments in the loaded facets. The bending stresses are dependent on the stiffness of the joints. Approximate solutions are developed to estimate the magnitude of the bending stresses. A FE-model of a facetted glass shell structure is used to validate the expressions and to give more detailed information about the distribution of the bending stresses.

Keywords: Structural glass, Shell structures, Facetted geometry, Plate bending

1. Introduction

The typical use of triangular and quadrangular facets in doubly curved facetted shells requires the use of triangulated truss systems or quadrangular truss framing with diagonals or cross tension cabling. In such a structure, the load carrying ability is based on forces concentrated in the framing system, while the glass merely serves as a separation between inside and outside. In this paper facetted glass shell structures with three adjoining edges in each vertex are investigated, since the load carrying ability of such a structure is achieved primarily by in-plane forces in the facets and the transfer of distributed in-plane forces across the joints, see [1] and [2]. This way it is the glass facets themselves, and not an added framing system, that carry the load. Such a geometry is called a plane-based geometry. An example is shown in figure 3.

A distributed load on a plane-based facetted structure will cause bending moments in the loaded facets. Via this bending, the load is transferred to the facet edges, and if the rigidity of the structure is adequate, the load is subsequently carried via membrane forces in the facets [3]. This discrete transformation of the load into membrane forces is basically what separates a facetted shell structure from a smooth shell structure, where the transformation of the load into in-plane forces happens continuously.

When using glass as the load carrying material, the brittleness of the material must be carefully considered in the design. An optimum would be a relatively low stress level, none or small stress concentrations, ductility through lamination and the choice of a structural system with redundancy in case of local failure. In this context, the facetted glass shell is an interesting choice. The stresses are well distributed over the facets, and support conditions can be chosen so a redistribution of stresses is possible in case of local failure. The only structural part needed besides the load carrying glass panes themselves is a joint that can transfer relatively small stresses between the facets.

In this paper, the focus is on bending stresses in the facets.

1.1. Bending moments in the facets

The magnitude and distribution of bending stresses in a plane-based shell structure can be determined by the use of a FE model of the structure, but this is a tedious and time consuming process for this specific type of structure. Therefore, a tool is needed to estimate the bending stresses in a conceptual design phase. Also, the possible existence and magnitude of local stress concentrations needs to be investigated.

In this paper an approximate solution is developed for determining the bending stresses in the facets, when the stiffness of the joints between the facets is varied. This solution is then validated through a case study. The case study is a FE-calculation of a facetted glass shell structure with a span of approximately 11 meters, and facets of about 2 meters in diameter.

2. Approximate expressions for the behaviour of a hexagonal plate

In a conceptual investigation each hexagonal plate can be viewed as simply supported and partially rotationally restrained by the connection to the neighboring plates. This partial restraint can be modeled as a elastic rotational spring, with a spring stiffness dependent on the joint design.

In the following the value of this rotation resistance will be estimated and its influence on the system investigated. The goal is to show how the edge rotation, the plate deflection and the surface stress perpendicular to the edge are linked, and determine these three variables, given a certain geometry, plate material and load.

The relation between joint stiffness and rotation of plate edges is interesting because we can estimate what level of rotational restraint is present, given an interval of physically believable values of joint stiffness.

Naturally, if the plates are clamped to each other this will lower the overall stresses in the plates and reduce the deflection, which is advantageous for the glass facets. However, the stresses in the joint are significantly larger when bending is transferred through them. Therefore, it is essential to know at what level of joint stiffness this rotational restraint becomes significant.

2.1. Conditions and assumptions

In the expressions below the hexagonal plates have been approximated by a circular plate. We thereby use a problem of rotational symmetry to approximate a much more complex problem. Effects such as varying torsional moments and out-of-plane shear forces, corner uplift effects, etc. are disregarded.

The effects of the plate rotations are assumed to decouple from shear deformations.

Membrane stresses in the plate are not considered in the expressions, and the plate bending is assumed to decouple from the in-plane effects (in accordance with linear plate theory).

It is assumed that the two plates meeting in a connection line, are loaded by a similar load, and have similar stiffness and support conditions. In other words, it is assumed that the impact on the joint is symmetric around the direction of the joint.

2.2. Derivation of approximate solution for plate behaviour

As described above a hexagonal plate has been approximated by a circular plate. The plate is loaded by a uniform load of q and simply supported along its edge. The expressions are linear and we have assumed small translations and rotations.

The circular plate has a diameter d, chosen so that its maximum deflection when simply supported is the same as the original hexagonal plate, when this is simply supported. The plate material has Young's modulus E and Poisson's ratio υ. The plate thickness is t.
The stiffness constant, c, ties the surface stress, σ, to the rotation around the edge direction, φ, as follows:

$$\sigma = c\varphi \tag{1}$$

where, φ is the rotation angle of the plate edge as illustrated in figure 1, and σ is the bending stress, perpendicular to the edge.

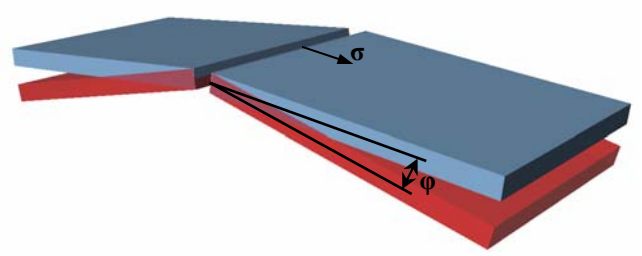

Figure 1: Rotation in joint. The red plate illustrates the deformed facet.

Deflection of the plate midpoint, u, normal stress at the plate surface, perpendicular to the edge, σ, and edge rotation, φ, are listed in table 1 for two different support conditions: The edge fully restrained against rotations as well as translations (index c for clamped) and the edge simply supported (index s).

Table 1: Analytical expressions for u, σ and φ [4]

Edges clamped	Edges simply supported
$u_C = \frac{1}{1024}\frac{qd^4}{D}$	$u_S = \frac{5+\upsilon}{1+\upsilon}\frac{1}{1024}\frac{qd^4}{D} = \frac{5+\upsilon}{1+\upsilon}u_C$
$\sigma_C = \frac{3}{16}\frac{qd^2}{t^2}$	$\sigma_S = 0MPa$
$\varphi_C = 0$	$\varphi_S = \frac{qd^3}{64D(1+\upsilon)} = u_S\frac{16}{d(5+\upsilon)}$
$\sigma_{midt,C} = -\frac{3}{32}(1+\upsilon)\frac{qd^2}{t^2}$	$\sigma_{midt,S} = -\frac{3}{32}(3+\upsilon)\frac{qd^2}{t^2}$

where

$$D = \frac{Et^3}{12(1-\upsilon^2)}$$

A linear interpolation between the two known solutions (edges clamped and simply supported respectively) are used to describe the edge rotation, φ, and bending stress perpendicular to the edge, σ.

$$\varphi = \varphi_S \frac{u - u_C}{u_S - u_C} \tag{3}$$

$$\sigma = \sigma_C \frac{u_S - u}{u_S - u_C} \tag{4}$$

We now have the information necessary to determine the three unknown variables, u, σ and φ. Using (1) and (4) to eliminate σ, substituting (3) and introducing φ_S from table 1, we get

$$u = u_C \frac{A + \frac{5+\upsilon}{1+\upsilon}}{A+1} \quad \text{where} \quad A = c \frac{16\, u_S}{(5+\upsilon)\, d\, \sigma_C} = c \frac{d}{t} \frac{1-\upsilon}{E} \tag{5}$$

Once the deflection is known, σ and φ are easily calculated.

In order to more easily interpret the results, a rotational restraint factor α is introduced. When $\alpha = 0$ there is no rotational restraint and $u = u_S$. When $\alpha = 1$ the plates are fully clamped together and $u = u_C$. We have

$$\alpha = \frac{u_S - u}{u_S - u_C} = \frac{A}{A+1} \tag{6}$$

when $u_S = \frac{5+\upsilon}{1+\upsilon} u_C$ is substituted into the expression. A is a constant that tells us something about the solution. If A is large (compared to 1), the deflection value approaches u_C and if A is close to zero the deflection approaches u_S. If $A = 1$, the deflection is exactly half way between u_C and u_S. The physical interpretation of this is that depending of the flexibility of the joint, the connection will behave somewhere in between simply supported and clamped. The value of A grows larger (and the solution thereby closer to a clamped plate) if the spring stiffness increases, if the plate size increases, or if the plate thickness decreases. The first condition is self-explanatory; a stiffer joint results in smaller rotations. The next two conditions states that the more flexible the plate is, the larger influence the connection stiffness has. This is also logical since a more flexible plate will try to rotate more at the edges, whereby "activating" greater resistance in the connection.

3. Estimated influence of the connection stiffness

In order to investigate the influence of the connection stiffness we need to determine a physically realistic region for the value of the connection stiffness. The starting point in the present investigation is the connection design shown in figure 2.

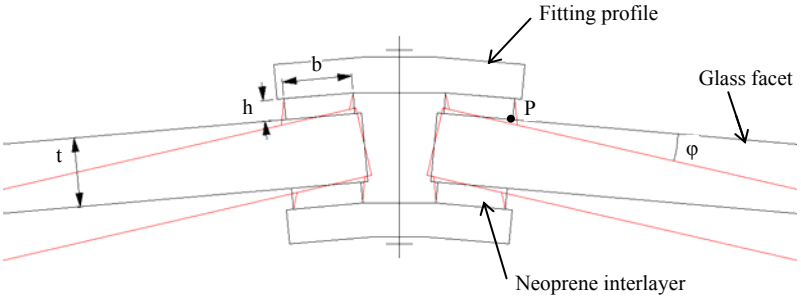

Figure 2: Connection design. The stiffness of the fitting profile is large compared the neoprene.

Here we have

$$\varepsilon_P = \frac{\varphi \cdot \frac{1}{2} b}{h} \ , \ \sigma_P = \varepsilon_P E_n$$

$$\gamma_P = \frac{\varphi \cdot \frac{1}{2} t}{h} \ , \ \tau_P \cong \gamma_P \frac{1}{3} E_n$$

where ε_P is the normal strain and γ_P is the shear strain in point P, φ is the rotation, E_n is Young's modulus for the interlayer (assuming that the material's behaviour is linear elastic under the considered circumstances, and that Poisson's ratio is close to 0.5) and b and h are the measures shown in figure 2. The total transferred moment to the glass plate is therefore

$$m_{tot} = 2 \cdot \frac{1}{6} \frac{\varphi \cdot \frac{1}{2} b}{h} E_n b^2 + \frac{\varphi \cdot \frac{1}{2} t}{h} \frac{1}{3} E_n \cdot bt$$

The stress in the glass from this moment:

$$\sigma = m_{tot} \frac{6}{t^2} = \varphi \underbrace{\left[\frac{E_n b^3}{h t^2} + \frac{E_n b}{h} \right]}_{C}$$

When likely minimum and maximum values of variables b (7mm to 12mm), t (8mm to 15mm), h (3mm to 5mm) and E_n (3MPa to 8MPa) are inserted into this expression, we get:

$$c \in \left[5MPa \ ; 100MPa \right]$$

Even though this is a rather large range of values, we shall see from an example below that the stiffness is at a level where it will result in a small rotational restraint factor, α. Since we know that a more flexible plate will result in higher level of rotational restraint, we choose a ratio between plate diameter and thickness which is quite high.

The material is glass with $E = 70 \cdot 10^3 MPa$ and $\upsilon = 0.22$. A plate diameter of 1.5m and a plate thickness of 10mm gives us

$$c \leq 80\,MPa\ , \quad A \leq 0.13$$

which yields:

$$\alpha = \frac{A}{A+1} \leq 0.12$$

This means that in a case of a very flexible plate combined with a very stiff joint only about 12% of the bending moment corresponding to a full rotational restraint will be transferred through the connection. A possible initial slip in the connection will reduce this value further.

4. Parameter study of stress distribution for varying joint stiffness

In the following the bending stresses in a facetted shell structure are investigated for different levels of rotational stiffness in the joints.

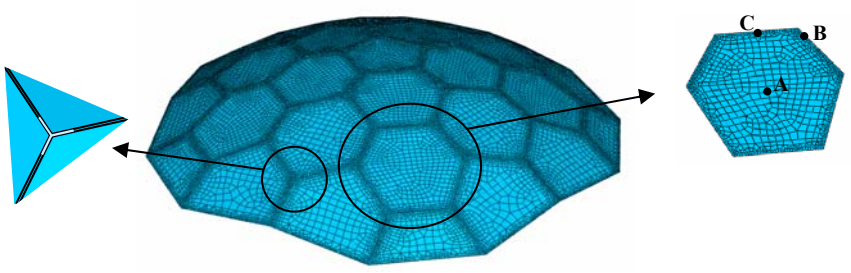

Figure 3: Facetted glass shell modelled in Abaqus. The image to the left shows the detail in the corner, where a much more flexible material replace the stiff joint along the first 10cm from the glass corner.

An example of a facetted shell structure of glass has been calculated in the finite element software Abaqus. The modelled structure is a convex plane-based facetted shell structure, where all facets are tangent planes to the same paraboloid of revolution, see figure 3. The maximum span is about 11 metres. The facets measure roughly 2 metres diagonally. The structure is supported against translation in all three directions along the boundary. The load is a uniform pressure load of $1.0 kN/m^2$ acting downward, perpendicular to the facets. The facets are all $10mm$ glass plates with a stiffness of $70GPa$. The joints between the facets are modelled as $10mm$ wide strips of elements with a stiffness ranging from $5MPa$ to $50MPa$. Along the first $10cm$ from each glass plate corner, the joint elements have been replaced by elements in a much more flexible material. The FE-model consists of thin shell elements, which do not include out of plane shear deformations. All calculations are linear, corresponding to small deformations.

Assuming that φ is small the stiffness of the joints are approximately related to the stiffness constant, c, by

$$c = \frac{\sigma}{\varphi} = \frac{\varepsilon E_j}{\varphi} = \frac{\frac{\varphi t}{b} E_j}{\varphi} = \frac{b}{t} E_j$$

where E_j is the stiffness of the joint material in the model. Since the joint width and thickness are both 10*mm* in the analysis, we can use E_j directly as a measure for the stiffness constant c.

Two series of analysis have been carried out, as shown in table 2.

Table 2: Overview of analysis series

	Analysis no.	Joint stiffness, continuous connection	Joint stiffness, corner area
Series 1	1	5MPa	0.1MPa
	2	10MPa	0.1MPa
	3	20MPa	0.1MPa
	4	30MPa	0.1MPa
	5	50MPa	0.1MPa
Series 2	6	20MPa	0.001MPa
	7	20MPa	0.1MPa
	8	20MPa	20MPa

The in-plane principal stresses are evaluated in three points shown in figure 3, i.e. in the middle of a facet (point A), at the glass edge where the stiff joint and the soft corner filling meet (point B), and on the glass edge at the middle of a joint line (point C). The principal bending stresses in these three points are illustrated in figure 4. The approximate solution for the bending stress is illustrated in the figure for point A and C.

4.1. Results from FE analysis series 1

As shown in figure 4 the stress in the middle of the facet (point A) is reduced about 10% when the joint stiffness increases from 5*MPa* to 50*MPa*, indicating a small increase in rotational restraint effect. The approximate solution for the variation of the bending stress is determined as derived in chapter 2, and plotted in the figure (point A). There is a good agreement between the approximate solution and the results from the FE calculation.

The membrane stress in the middle of the facet (not illustrated) is about 0.5*MPa* and does not change notably when the joint stiffness is varied, indicating that the overall linear elastic shell behaviour is not affected by the rotational stiffness of the joints.

In point B, where the load transferring joint meets the soft corner filling, and where there is a risk of a stress concentration because of the sudden change of stiffness, only a moderate stress increase can be observed when the stiffness of the joint is increased; A stress concentration in this point appears not to be a problem for the studied problem.

At the middle of the joint (point C) the minimum principal stress, S2, increases in magnitude when the joint stiffness decreases. The direction of the minimum principal stress is the edge direction. Larger flexibility of the joint allows for an increasing curvature of the supported edge. The largest value of S2 does not exceed the largest stress in the facet as a whole, and is therefore not a design problem.
In point C the maximum principal stress, S1, is oriented perpendicular to the edge, and therefore directly shows the bending stress from the rotational restraint effect in the joint. The approximate solution for the bending stress is shown in the same illustration (point C). The approximate values have been corrected for the eccentricity of the glass edge relative to the symmetry plane, which is the middle of the joint.

4.2. Results from FE analysis series 2

In analysis series 2 the stiffness of the corner filling has been varied. The results are not shown here, but are briefly described in the following.
The most interesting conclusion to draw from the results is that the transition from stiff joint to soft joint does not result in stress concentrations that are significantly larger than the stresses present when there is no discontinuity in the stiffness (i.e. when the stiffness of the corner filling is 20*MPa*, like the joint itself). However, a stiff joint material in the corner area gives rise to other stress concentrations, which are more thoroughly described in [3]. Since a stiff joint in the corners does not contribute to the stiffness of the structure, but on the contrary gives rise to unnecessary stress concentrations, it is preferable to use a soft filling in the corner areas, e.g. a wet silicone.

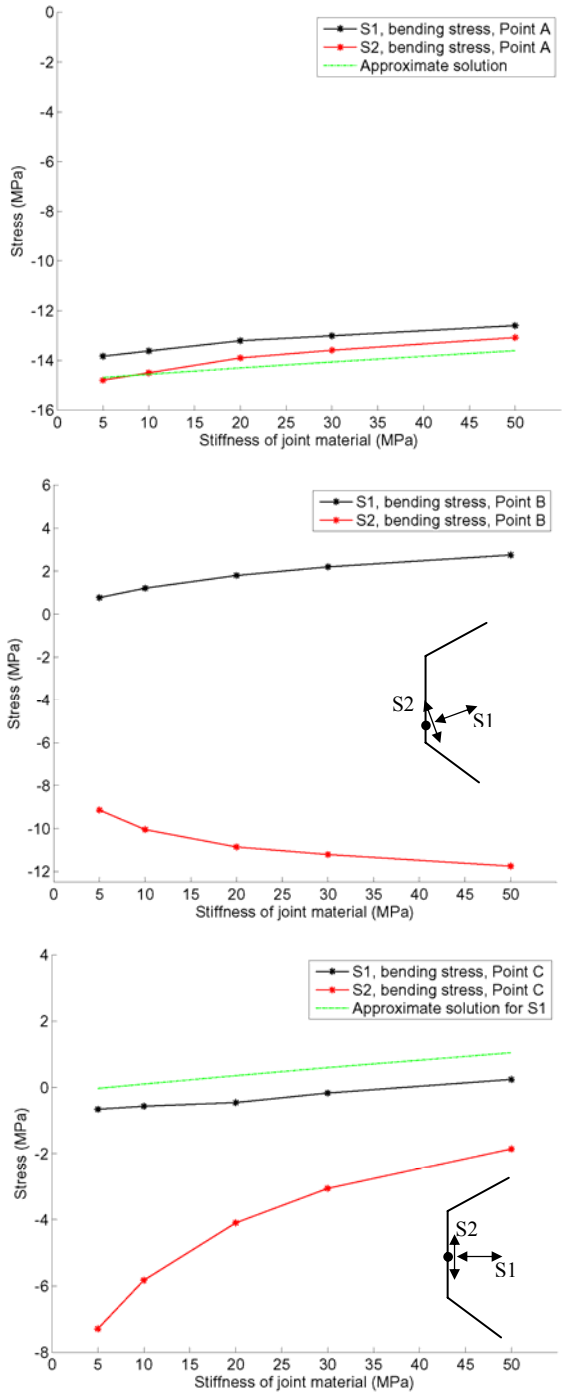

Figure 4: Bending stress in the three evaluated points. Analysis series 1.

5. Conclusion and discussion

For a joint stiffness similar to that of the joint shown in figure 2, a good estimation of the bending behaviour in a facet can be attained by determining the rotational restraint factor α given by (6). This factor gives us information about how much the rotational stiffness of the joints affects the support conditions of the facets.

The case study in Abaqus showed no indication of significant stress concentrations in any part of the facet for the tested range of joint stiffness. The maximum bending stress occur in the middle of the facet.

A linear relation has been assumed between rotation and resistance against rotation in the connection. This is probably violated by an initial slip in the physical connection. The rotations are typically very small – with deformations less than half a millimeter in the joint – and therefore even a slight slip will have a large impact on the rotational constraint, and thereby also on the validity of the estimation of α. The consequence will be that the plate in reality is closer to simply supported than estimated by the rotational restraint factor, α.

The case study was modeled in Abaqus with focus on attaining the correct rotational stiffness in the joint. However, also the shear stiffness (out-of-plane as well as in-plane) and the axial stiffness perpendicular to the joint line, influence the stress distribution, and it has not been investigated how well these values are represented by the modeled strip of joint elements. It should be evaluated how well these other stiffness effects are represented. If it is deemed necessary, another set of variables in the joint (a combination of width, thickness, stiffness and Poisson's ratio) can be combined to represent the same rotational stiffness but at the same time a more physically correct shear- and axial stiffness.

6. References

[1] Wester, Ture, *Structural Order in Space – the plate-lattice dualism,* The Royal Danish Academy of Fine Arts, School of Architecture, Smed Grafik, 1984.

[2] Bagger, Anne; Jönsson, Jeppe; Almegaard, Henrik; Wester, Ture, *Facetted Shell Structure of Glass*, Glass Processing Days, Conference Proceedings, Tampere, 2007.

[3] Bagger, Anne; Jönsson, Jeppe; Wester, Ture, *Investigation of Stresses in Facetted Glass Shell Structures*, International Association of Shell and Spatial Structures (IASS) Symposium, Conference Proceedings, Venice, 2007.

[4] Timoshenko, S.P.; Woinowsky-Krieger, S., *Theory of Plates and Shells*, McGraw-Hill, N.Y., 1959